Infrared spectral marker bands characterizing a transient water wire inside a hydrophobic membrane protein

Steffen Wolf, Erik Freier, Qiang Cui, and Klaus Gerwert

Citation: The Journal of Chemical Physics **141**, 22D524 (2014); doi: 10.1063/1.4902237
View online: http://dx.doi.org/10.1063/1.4902237
View Table of Contents: http://scitation.aip.org/content/aip/journal/jcp/141/22?ver=pdfcov
Published by the AIP Publishing

Infrared spectral marker bands characterizing a transient water wire inside a hydrophobic membrane protein

Steffen Wolf,[1,2] Erik Freier,[2] Qiang Cui,[3] and Klaus Gerwert[1,2,a)]
[1]*Department of Biophysics, Ruhr-University Bochum, Universitätsstraße 150, 44780 Bochum, Germany*
[2]*Department of Biophysics, Chinese Academy of Sciences, Max-Planck-Gesellschaft Partner Institute for Computational Biology, 320 Yue Yang Road, 200031 Shanghai, China*
[3]*Department of Chemistry and Theoretical Chemistry Institute, University of Wisconsin, Madison, 1101 University Avenue, Madison, Wisconsin 53706, USA*

(Received 15 September 2014; accepted 10 November 2014; published online 25 November 2014)

Proton conduction along protein-bound "water wires" is an essential feature in membrane proteins. Here, we analyze in detail a transient water wire, which conducts protons via a hydrophobic barrier within a membrane protein to create a proton gradient. It is formed only for a millisecond out of three water molecules distributed at inactive positions in a polar environment in the ground state. The movement into a hydrophobic environment causes characteristic shifts of the water bands reflecting their different chemical properties. These band shifts are identified by time-resolved Fourier Transform Infrared difference spectroscopy and analyzed by biomolecular Quantum Mechanical/Molecular Mechanical simulations. A non-hydrogen bonded ("dangling") O–H stretching vibration band and a broad continuum absorbance caused by a combined vibration along the water wire are identified as characteristic marker bands of such water wires in a hydrophobic environment. The results provide a basic understanding of water wires in hydrophobic environments.
 [http://dx.doi.org/10.1063/1.4902237]

I. INTRODUCTION

Wires of protein-bound water molecules are essential features in proton transporting membrane proteins.[1] These proteins, such as PS II,[2–4] cytochrome C oxidase,[5–7] respiratory complex I,[8] and the bacterial reaction center,[9,10] are crucial in the maintenance of a transmembrane proton gradient necessary for ATP synthesis.[11] Opposed to the situation in bulk water,[12,13] these protein-bound water wires conduct protons from the protein surface to the proteins' active sites, or through the protein core across a membrane, in directional transport mechanisms.[14] Moreover, protein-bound water molecules are discussed to be key players in proton conduction through the human Hv1 proton channel,[15,16] channelrhodopsin II,[17,18] which is the corner stone of optogenetics,[19] and the M2 proton channel of influenza viruses, which is an important target for antiviral drugs.[20,21] Quite the opposite of these systems, aquaporins selectively transport water molecules in form of similar chains, but inhibit proton transport along them.[22] Rearrangements of protein-bound water molecules were also found in the activation process of several G protein-coupled receptors (GPCRs).[23–27] Protein-internal water molecule positions observed in different GPCR crystal structures are conserved, pointing to a highly conserved water-mediated activation mechanism.[28] Water molecule networks therefore are as important as amino acids for the function of transmembrane proteins.[1,14] Understanding their dynamics, properties, and structure is a crucial prerequisite for understanding protein function.

Water molecules within the core of a protein may face hydrophobic surfaces.[29–32] This situation strongly resembles the one of water molecules found in single walled narrow carbon nanotubes:[33,34] here as well, water molecules have to form a linear chain through a narrow hydrophobic tube without being able to form hydrogen bonds with the surrounding hydrophobic walls. As a result, both protein-bound and carbon nanotube-bound water wires clearly differ in their physicochemical properties from bulk water. A targeted change in nanotube-bound water wire composition has been proposed as basis for, e.g., protonic current-based field-effect transistors.[33] Thus, studying the mechanisms of proton transfer through protein-bound water wires is a source of information for understanding proton transfer in membrane proteins and also for the creation of new nanoscale devices.

The physicochemical changes are best reflected in the vibration properties of the investigated water molecules: missing hydrogen bond partners lead to so-called "dangling" O–H bonds, which exhibit blue shifted O–H stretch vibrations.[14] Furthermore, within proteins, charges from amino acid side chains cause strongly polarized and thus elongated hydrogen bonded O–H bonds, leading to red shifted O–H stretch vibrations. These altered O–H bond vibrations should provide excellent infrared marker bands to track the transient formation and destruction of protein-internal water networks. However, protein-bound water wires and networks are highly dynamic and in some cases only transiently existing. They therefore need to be investigated by methods with a high time resolution. Here we demonstrate that by combining time-resolved FTIR spectroscopy and coupled Quantum Mechanical/Molecular Mechanical (QM/MM) simulations, we are able to

a)Author to whom correspondence should be addressed. Electronic mail: gerwert@bph.rub.de.

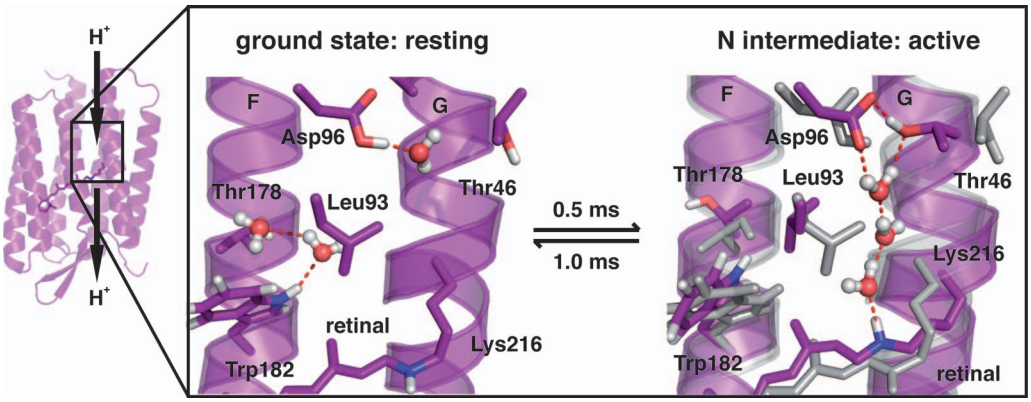

FIG. 1. Proposed water wire formation at the proton uptake site of bacteriorhodopsin.[1,35] Helices F and G shown as cartoon, relevant amino acid side chains and retinal cofactor in sticks, water molecules as balls and sticks. Ground state protein conformation indicated in grey on right side for comparison. A conformational change of the retinal cofactor affects the conformation of Trp182, Thr178, and Leu93. This conformational change removes hydrogen bond contact sites for protein-bound water molecules, which are located at two different resting storage sites. In the following, they move over towards active positions close to helix G and form a linear chain, bridging Asp96, and the retinal Schiff base. Along this water wire, the proton stored at Asp96 is transferred via Grotthuss transfer[12] to the Schiff base of the retinal cofactor and Lys216.

identify and track such marker bands of transient water wires in a membrane protein with a high time resolution and thus follow the formation of protein-bound water motifs. Furthermore, we show that the marker band line shape is directly coupled to the structure and dynamics of the respective water network, which allows the elucidation of its transient structure at atomic detail.

To demonstrate our strategy, we study bacteriorhodopsin (bR),[36] a light-driven proton pump from the protein family of microbial rhodopsins.[37] Like all microbial rhodopsins, it contains a retinal chromophore, which is covalently bound to the protein via a protonated Schiff base. Upon light activation, the chromophore undergoes isomerisation and protonation/deprotonation reactions, which drive the protein through a cycle of well-defined intermediate conformations[36] termed K, L, M, N, and O, in order of their appearance. The general importance of water molecules in the proton transport in bR was elucidated in detail.[1,14,38,39] However, only recently, we found the putative IR spectral signatures of a proton transporting water wire within the N intermediate of the proton pumping photocycle of bR.[35] Figure 1 depicts the proposed water wire formation mechanism herein: water molecules are moved by defined conformational changes from their inactive ground state storage positions into the hydrophobic proton uptake region to form a transient wire between Asp96 and the Schiff base nitrogen atom. By a proton transfer from Asp96 to the Schiff base, the central proton binding site at the Schiff base is reprotonated. We experimentally identified the spectral signatures of two "dangling" water molecules at 3670 cm^{-1} and 3658 cm^{-1}.[14,35] Dangling water molecule vibrations can be observed in the same IR spectral regime in carbon nanotube-bound water wires, too.[40] Furthermore, we observed a broad continuum absorbance band between 2750 cm^{-1} and 2540 cm^{-1}. We attributed these two spectral features to a transient water wire of three water molecules, transiently bridging Asp96 and the retinal Schiff base in the N intermediate. In this article, we explicitly disentangle the unusual vibrational characteristics of this transient water wire by QM and QM/MM simulations and compare the computed IR spectra with experimentally derived FTIR spectra.

II. COMPUTATIONAL METHODS

A. Normal mode analysis (NMA)

NMA was carried out in GAUSSIAN09.[41] The calculations were based on our 20 ns membrane equilibrated structures from our earlier simulations with a bR trimer, of which one protein was modeled to be in the N state.[35] To represent a minimum of different conformations of the water wire and its surrounding amino acids, three independent sample runs were carried out for each system, each basing on different and randomly chosen time steps during the last 5 ns of these earlier MM simulations. The vacuum models contained the Thr46, Asp96, and Lys216 side chains, the retinal cofactor, and the water molecules found between those residues. Systems were prepared for vacuum calculations so that amino acids backbone atoms were removed, with the exception of C(alpha), and retinal was capped between C11 and C12. The resulting QM vacuum models contained 62 atoms in total (39 hydrogen atoms, 16 carbon atoms, 6 oxygen atoms, and 1 nitrogen atom). A full overview of a representative QM vacuum model is given in Figure S1 in the supplementary material.[42] Due to SCF convergence problems, we performed a three-step minimization process: The systems were initially optimized at the HF level with a 6-31+G* basis set and the Berny algorithm using GEDIIS[43] as SCF procedure. We then continued with a B3LYP optimization with a 6-31++G** basis set and a quadratic convergent SCF procedure,[44] followed by a last round of B3LYP optimization with a 6-31++G** basis set and GEDIIS as SCF procedure. To keep the current side chain orientation in the respective snapshots, all C(alpha) atoms, the C(delta) atom of Asp96, the retinal C12, and the Schiff base nitrogen atom were constrained to their initial positions during the full minimization sequence (see Figure S1 in the supplementary

material[42]). Normal mode calculation was then performed using B3LYP with a 6-31++G** basis set by diagonalization of the Hessian matrix of the QM system. Asymmetry corrected vibrations were calculated by an asymmetry factor of 0.9632.[45]

B. Self-consistent charge density functional tight-binding (SCC-DFTB) calculations

QM/MM simulations were carried out using the Chemistry at HARvard Molecular Mechanics (CHARMM) program (c33b1 version)[46] with the CHARMM22 force field,[47] and TIP3P water molecules.[48] WT bR simulations were based on the membrane-equilibrated bR N intermediate structural model from our earlier simulations mentioned above[35] after 20 ns of simulated time. V49A mutant calculations are based on the 1.62 Å N′ structure by Schobert *et al.* (PDB ID 1P8U).[49] Missing hydrogen atoms were added with HBUILD.[50] Asp85, Asp115, and the Lys216-retinal Schiff base were set to be protonated.[51] An all-trans-retinal topology was obtained from Refs. 52 and 53. For water molecule addition, we extracted water molecules from the final membrane/solvent simulation structure with a distance of 25 Å to the NZ atom of Lys216 and added missing water molecules by superimposing the system with a water sphere of 25 Å. We used the generalized solvent boundary potential (GSBP) approach[54,55] to account for electrostatics, with parameters and workflow as previously done by Goyal *et al.*:[56] the system was partitioned into a 22 Å inner region centered at the NZ atom of Lys216, while the rest of the protein was treated as the outer region.

For QM/MM simulations, we used the third-order extension of SCC-DFTB[57,58] plus the modification of the γ function for atom pairs involving hydrogen.[58] To achieve SCF convergence, the electron temperature was set to 500 K. The Quantum Mechanics (QM) boxes contained the Asp96 and Lys216 side chains, the retinal cofactor, and the water molecules found between those residues. Thr46 had to be excluded from the QM box, as its inclusion blocked SCF convergence during calculation. The QM/MM boundary was accounted for by introducing link-atoms between the Cα and Cβ atoms of the QM amino acids.[59] All QM/MM simulations mentioned below were carried out with a step size of 0.5 fs, solving Newton's equations of motion for the MD region within 18 Å of the NZ atom of Lys216. Motions in the buffer region (18–22 Å) were calculated by Langevin dynamics with a temperature bath of 300 K.[60] To keep them inside the inner sphere, water molecules were subjected to a weak GEO-type restraining potential as described in Goyal *et al.*[56] All protein atoms in the buffer region were harmonically restrained with force constants: these B factors were directly determined with the g_rmsf module of GROMACS[61] from the protein dynamics during the last 5 ns of trajectories presented in Freier *et al.*[35] To account for protein groups and water molecules that switched between inner and buffer region during simulations, Langevin atoms were updated heuristically. Within the inner sphere we used an extended electrostatics model, in which groups beyond 12 Å interact as multipoles.[62] The entire system was minimized via the Adopted Basis Newton-Raphson method available in CHARMM, then heated gradually to 300 K, and then directly subjected to production runs.

Theoretical IR spectra were computed by the Fourier transform of the classical dipole autocorrelation function (FT-DAC)[63,64] as described in Goyal *et al.*[56] No SHAKE constraint[65] was applied to any bond. For each system with different QM box size, three independent trajectories (same starting coordinates, different temperature seeds) with a length of 1.1 ns each were carried out for each setup for spectra calculation. The dipole moment was calculated on-the-fly from the coordinates and Mulliken charges of QM atoms at each step. The IR spectrum for the QM region were then computed by the Fast Fourier transform of the dipole autocorrelation function of such dipoles, using 2097152 data points, and a Blackmann filter to enhance spectral resolution. For facilitating spectral comparison and further enhancement of the signal-to-noise ratio, spectra from the three separate runs for each QM box size were averaged into one spectrum, which then was smoothed by calculating its running average with a window size of 16 cm^{-1}. As mentioned in the main text, we here focus on comparison of the spectral line shape, but not the exact spectral position, as SCC-DFTB exhibits frequency inaccuracies of up to 200 cm^{-1} for O–H vibrations.[66] We therefore rescaled the calculated spectra such that the calculated dangling vibrations of the three water molecule wire at 3807 cm^{-1} (assignment was done in comparison with NMA modes given in Table SI in the supplementary material[42]) matches the experimentally observed double peak at 3670 cm^{-1} and 3658 cm^{-1} (the unscaled spectra can be seen in Figure S2 in the supplementary material[42]). This resulted in a scaling factor of 0.962. As we obtain this scaling factor by matching the calculated dangling O–H stretch vibrations with the experimental ones, we expect the factor to be applicable to other O–H stretch vibrations, as well. This is justified by the resulting nice match of experimental and theoretical spectra of the broad continuum absorbance between 2775 cm^{-1} and 2525 cm^{-1}. To facilitate spectral comparison of combination vibration bands between 3000 cm^{-1} and 2500 cm^{-1}, we corrected the respective spectral range by subtracting an exponential function from the calculated spectra. This exponential function mimics temporally uncoupled O–H vibrations of single water molecules in the water wires (comparable to vibrations in bulk water), which we observed in calculations with a QM box consisting out of only Asp96 and the water molecules (see Fig. S3 in the supplementary material[42] for the respective spectra and correction functions). Though these calculations contain an excess charge of −1, Goyal *et al.* showed that the resulting spectra show a neglectable coordinate dependence,[56] and thus can be compared with the ones obtained from QM boxes, which additionally include the retinal Schiff base. For calculations with a water wire out of three water molecules, the exponential function had the form of

$$y[\text{a.u.}] = 7.5363 \times 10^{-7} \exp(6.1378 \times 10^{-3} x[\text{cm}^{-1}]). \quad (1)$$

For the systems with a water wire of four water molecules and V49A, the exponential function had the form of

$$y[\text{a.u.}] = 8.4 \times 10^{-7} \exp(6.1398 \times 10^{-3} x[\text{cm}^{-1}]). \quad (2)$$

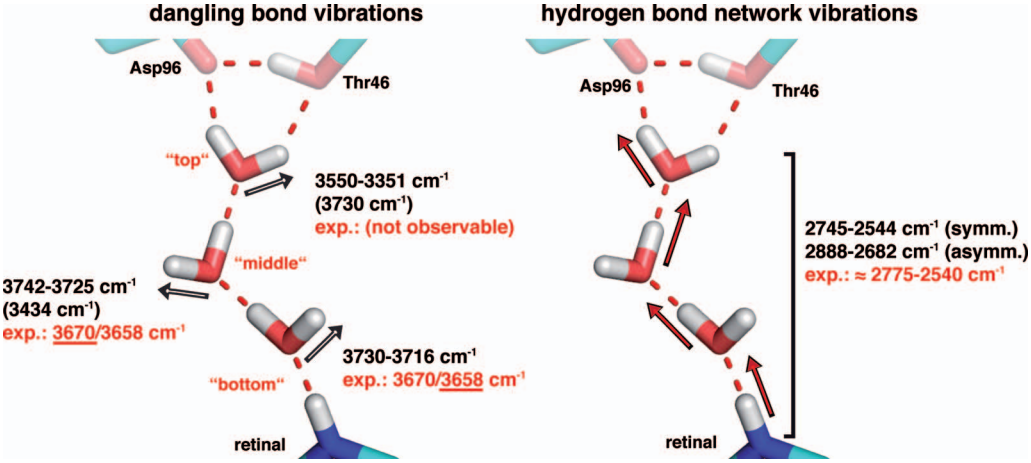

FIG. 2. Normal mode frequency analysis (NMA) of the polarized water wire vacuum QM model (see Table SI in the supplementary material[42]) compared to experimentally determined absorptions.[35] The analysis reveals two groups of dangling O–H bonds: two bonds with frequencies between 3742 cm^{-1} and 3716 cm^{-1} at the water molecules termed "middle" and "bottom," and one bond with a frequency around 3350 cm^{-1} at the water molecule termed "top." Frequencies in brackets denote a situation where the hydrogen bond arrangement has changed in a way that the "top" water molecule contains a dangling bond, while the "middle" water has none. The calculated dangling bonds are in agreement with the respective experimentally observed bands at 3670 cm^{-1} and 3658 cm^{-1}.[35] The hydrogen bonded O–H bonds of all water molecules and the N–H bond of the retinal Schiff base show combined symmetrical vibrations between 2745 cm^{-1} and 2544 cm^{-1}, and combined asymmetric vibrations between 2888 cm^{-1} and 2682 cm^{-1}. The symmetric vibrations are found within the range of the experimentally observed continuum band between 2775 cm^{-1} and 2540 cm^{-1}.

III. RESULTS AND DISCUSSION

A. Normal mode analysis

To gain a first understanding of the frequency range sampled by a water wire between Asp96 and the Schiff base, we carried out normal mode analyses (NMA) of DFT calculations with vacuum water wire model systems based on extracted snapshots from our earlier Molecular Mechanics (MM) MD simulations in a membrane/solvent environment.[35] Figure 2 depicts the result of this analysis (the detailed structures and frequencies for these models are summarized in Table SI in the supplementary material[42]). In agreement with our measurements in the IR regime of dangling O–H bonds, the water wire contains two water molecules (usually "middle" and "bottom"), which show dangling vibrations between 3742 cm^{-1} and 3716 cm^{-1}. As can be seen in Fig. 2, the absorption ranges of both water molecules overlap to a large extent but are not completely identical (3730–3716 cm^{-1} and 3742–3725 cm^{-1}). This fits well with the experimentally observed vibrations at 3670 cm^{-1} and 3658 cm^{-1}, which form a double peak of two overlapping absorption peaks.[35] The calculated absorptions exhibit an acceptable blue shift of about 70 cm^{-1} to their experimental equivalents, possibly due to the vacuum environment of the model. The third water molecule (usually "top") is hydrogen bonded to both Thr46 and Asp96. It consequently exhibits no dangling vibration, but vibrations at 3550–3351 cm^{-1}; these overlap with the spectral range of bulk water and are therefore masked in the experimental time-resolved FTIR spectra. Due to the flexibility of the water molecules during the MD, the "top" and "middle" water molecules can switch one hydrogen bond partner (Thr46), leading to an alternative hydrogen bond pattern. This case (Table SI in the supplementary material,[42] conformation C) nonetheless exhibits the same spectral pattern of two "dangling" vibrations and one vibration masked by bulk water.

Within the range of strongly hydrogen bonded O–H vibrations, the vacuum model systems displayed in Fig. 2 show combined symmetrical vibrations between 2745 cm^{-1} and 2554 cm^{-1}, which is in very good agreement with the experimentally observed vibration between 2750 cm^{-1} and 2540 cm^{-1}, and combined asymmetric vibrations between 2888 cm^{-1} and 2682 cm^{-1}. Interestingly, these vibrations are not located on a single O–H bond, but arise from combined stretch vibrations of all hydrogen bonded O–H bonds of the three water molecules together with the N–H bond of the retinal Schiff base. The exact frequency of this vibration should therefore be very sensitive to the position of the water molecules. This fits to the experimentally observed broadening of the band over 210 cm^{-1} (see Fig. 3).

A linear chain of water molecules therefore indeed exhibits marker bands within the experimentally proposed spectral ranges. However, peak absorbances calculated in NMA analysis in the regime of strong hydrogen bonded O–H bonds cannot be directly compared with the experimentally observed broad continuum absorbances. To make such a comparison, we have to perform a calculation of the actual line shape of the IR spectra for the investigated water wire. For this, we need to employ a QM method that allows simulations long enough to sample its conformational range and dynamics. We therefore carried out third-order SCC-DFTB[57,58] QM/MM calculations and calculated the respective IR spectra by a Fourier transformation of the dipole autocorrelation function of the QM box.[66]

B. SCC-DFTB calculations

Figure 3 shows the theoretical spectra derived from SCC-DFTB QM/MM calculations of the water molecule wire in comparison with the experimental spectra. We here focus on comparison of the spectral line shape, but not the exact spectral position of the calculated absorbances, as SCC-

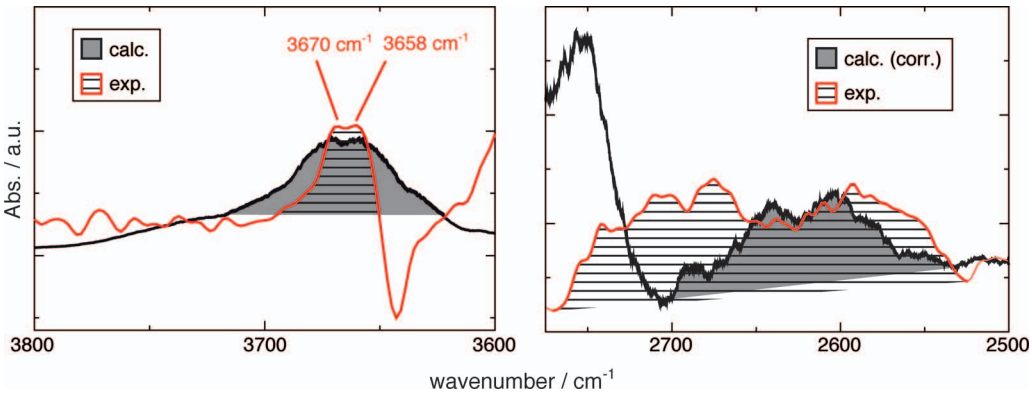

FIG. 3. Spectral signatures of the water wire calculated with SCC-DFTB QM/MM simulations in comparison with experimentally obtained BR-N spectra. Experimental spectra are in red and calculated spectra are in black. Frequencies were scaled by a factor of 0.962 to match calculated and measured dangling bond vibrations (see Materials and Methods and Fig. S2 in the supplementary material[42] for details). (Left) Dangling O–H bond range. The experimental spectrum shows a peak (hatched with horizontal lines) with two maxima at 3670 cm^{-1} and 3658 cm^{-1}, which was attributed to two water molecules with dangling O–H bonds appearing in the water wire.[35] In agreement with this, the simulations show one major combined absorption peak (highlighted in grey). The negative experimental peak at 3643 cm^{-1} is caused by a water molecule with a dangling O–H bond at the complex counter ion of the Schiff base.[14] (Right) Baseline-corrected strong hydrogen bond range. The experimental spectrum shows a broad double-hump shaped continuum absorbance feature between 2775 cm^{-1} and 2525 cm^{-1}. In agreement with this, the calculations result in a similar broad double-hump shaped continuum absorption feature between 2700 cm^{-1} and 2530 cm^{-1}.

DFTB exhibits frequency inaccuracies of up to 200 cm^{-1} for O–H vibrations.[66] We attribute the difference in peak position between the calculated and the measured dangling bond absorbances to SCC-DFTB being based on a minimal base set approach:[57] As such a minimal base set cannot respond well to polarization effects by surrounding charges, the stretch vibrations will not be affected by the protein environment *in silico* as much as in the real protein *in vitro*. As this should lead to a systematic error of the calculations, we decided to rescale the calculated spectra such that the calculated dangling vibrations of the three water molecule wire matches the experimentally observed double peak at 3670 cm^{-1} and 3658 cm^{-1} (see Materials and Methods and Fig. S2 in the supplementary material[42] for details), resulting in a scaling factor of 0.962. We assigned the spectral sources of the peaks by comparison with our NMA analysis from the vacuum models. In the range of dangling water vibrations, a single absorbance peak at 3665 cm^{-1} is observed. This peak fits well to the narrow shape of the experimentally observed double peak at 3670 cm^{-1} and 3658 cm^{-1}. As our NMA analysis showed, the vibrations of both "middle" and "bottom" water molecules cause this experimentally observed absorption. In agreement with this, a Fourier analysis of the frequency range of O–H vibrations of the water wire forming molecules (see Fig. S5 in the supplementary material[42]) show that both "middle" and "bottom" water molecule in SCC-DFTB calculations vibrate in this frequency range, too. An additional peak at 3552 cm^{-1} in the calculations (see Fig. S6 in the supplementary material[42]), coming from the "top" water molecule, would experimentally be masked by bulk water absorptions. In summary, the line shape of the dangling O–H bond spectral regime is in good agreement with the experimentally observed absorbance and therefore confirms the presence of a transient water wire in the N intermediate.

In the regime of strong hydrogen bonds, the scaled water wire spectra calculated via SCC-DFTB exhibits a broad double-hump shaped continuum absorption feature between 2700 cm^{-1} and 2530 cm^{-1}. Its shape closely resembles the experimentally observed broad double-hump shaped continuum absorbance between 2750 cm^{-1} and 2540 cm^{-1}. Though applying the scaling factor obtained from the dangling O–H bond regime, the minimum observed in the experimental spectrum at 2626 cm^{-1} agrees well with the scaled calculated minimum at 2624 cm^{-1} (see Fig. S6 in the supplementary material[42]), supporting our approach of scaling by a constant factor. As in the case of the dangling bond stretch vibrations, we attribute the difference in broadness between the calculated and the measured continuum absorbance to the minimal base set approach of SCC-DFTB: as polarization effects should be underestimated, the calculated continuum absorbance is more narrow than the measured continuum absorbance. Like in the case of the dangling O–H bond regime, the spectral line shape in the combined O–H vibration regime is in good agreement with the experimental line shape and thus agrees with the presence of a transient water molecule wire.

We here need to point out that the QM part of our QM/MM calculations does not contain the functionally important Thr46 side chain.[35,67] Inclusion of Thr46 into the QM part of QM/MM simulations always resulted in a crash of the QM/MM simulations due to missing SCF convergence. However, we found that there is a good match between the full QM vacuum model NMA spectra and the reduced model SCC-DFTB spectra, so we decided to keep Thr46 in the MM part. We therefore decided that despite its importance for both the photo cycle and water wire formation,[35,67] the influence of Thr46 on solely the IR spectrum of the water wire seems to be small enough to be neglected.

As an additional test, we investigated if a mutation of an amino acid forming the hydrophobic cavity of the water wire affects the calculated vibrations. Such a mutation is the V49A variant of bR, which forms the basis of a N′ intermediate crystal structure,[49] and was shown to affect the experimentally observed N intermediate continuum band.[35] Figure S6 in the

supplementary material[42] shows the resulting calculated spectra for V49A mutated bR: In the regime of strongly hydrogen-bonded water molecules, the mutant clearly misses the broad continuum absorbance feature, but exhibits a slope-like line shape comparable to the spectral signature of the four water molecule chain. Furthermore, in the regime of dangling O–H bonds, the V49A mutant exhibits a strongly altered line shape, with calculated absorptions ranging from 3550 cm^{-1} up to 3750 cm^{-1}. The structural reason for this change in line shape can be seen in Fig. S7 in the supplementary material:[42] the V49A mutation creates enough space to allow the intrusion of two additional water molecules between Asp96 and the Schiff base, which leads to a water chain made out of five water molecules. As the V49A mutant exhibits a strongly altered photocycle,[49] we need to verify the spectral changes with another mutant. Such a suitable mutation is Val49 to methionine: this mutation also affects the line shape of this absorbance.[68] Summing up, a mutation of an amino acid flanking the water wire exhibits changes of the calculated spectral line shape, which is in good agreement with experimental observations. This again highlights the sensitivity and quantitative nature of our strategy that combines experimental FTIR and theoretical spectra calculations.

C. Structural analysis of water wires

Having identified spectral marker bands indicative for protein-internal water wires, we wanted to verify if structural information can be obtained directly from their line shape. Figure S8 in the supplementary material[42] and Table SI in the supplementary material[42] show a normal mode analysis of an alternative four water wire model in the N state of bR.[35] Here as well, combined symmetrical stretch vibrations are found between 2734 cm^{-1} and 2626 cm^{-1} and dangling vibrations between 3740 cm^{-1} and 3555 cm^{-1}. The NMA therefore does not discriminate between water wires of different lengths. As Figure S8 in the supplementary material[42] shows, SCC-DFTB simulations with four water molecules only result in a broad unspecific absorption between 3750 cm^{-1} and 3625 cm^{-1}, which is not in agreement with the FTIR experiment. In the regime of strong hydrogen bonds, the four water molecule wire SCC-DFTB spectrum exhibits a slope-like shape above 2750 cm^{-1}, which does not agree with experimental spectra, too. The spectral line shape in both the dangling O–H bond regime and in the combined O–H vibration regime therefore is characteristic of a three-water molecule wire. By combining theory and experiment, we therefore are able to establish unambiguously the number of water molecules in a protein-bound internal water wire as well as the structure and dynamics of the underlying hydrogen bond network. Therefore, this strategy is especially interesting for proteins, where highly mobile water molecules are thought to participate in transient chain formation, which is difficult to observe with X-ray crystallographic analysis. For example, in high-resolution crystal structures of the bacterial reaction center, a water wire of eight water molecules can be resolved. A ninth water molecule was predicted at a position essential for proton transfer to the quinone cofactors,[10,69] but it was not observed in the respective crystal structures. Furthermore, continuum bands in the regime of strong hydrogen-bonded O–H stretch vibrations were observed to appear transiently in the protein reaction cycle.[69] Here, FTIR in combination with theoretical calculations can verify such predictions.

IV. CONCLUSION

By a close integration of time-resolved FTIR spectroscopy and different QM-based simulation techniques, we investigated the dynamic structure of a transiently formed water wire made out of protein-bound water molecules, which in the resting state are stored at inactive positions. During the proton-pumping cycle, this transient water wire allows a proton to pass through a hydrophobic environment in an intermediate protein conformation of a membrane protein. The water wire itself proves to be a highly polarized chain of water molecules passing through a narrow hydrophobic tube, and by this closely resembles the situation of water molecules passing through a single-walled carbon nanotube,[33,34,40] allowing the transfer of our findings to the development of nanoscale technical applications. This comparability implies that proton conduction through protein-bound water wires will be performed by a mechanism in form of intermediary Zundel ion-like steps.[70] We were able to determine spectral marker bands of such transient water wires. Figure 4 shows the spectral marker bands, which we found to be characteristic of protein-internal water wires: Between 3800 cm^{-1} and 3600 cm^{-1}, sharp absorption peaks can be observed, coming from dangling O–H stretch vibrations. Between 2900 cm^{-1} and 2500 cm^{-1}, broad continuum absorptions are observed, coming from combined stretch vibrations along the line of O–H bonds and hydrogen bonds, which together form the water wire. As these two spectral ranges are found outside of the bulk absorption range, they are highly specific spectral markers to track the transient appearance of such water wires. The IR line shape in these spectral regimes appears characteristic of the structure and dynamics of the water wire, allowing a detailed structural analysis, and even the determination of

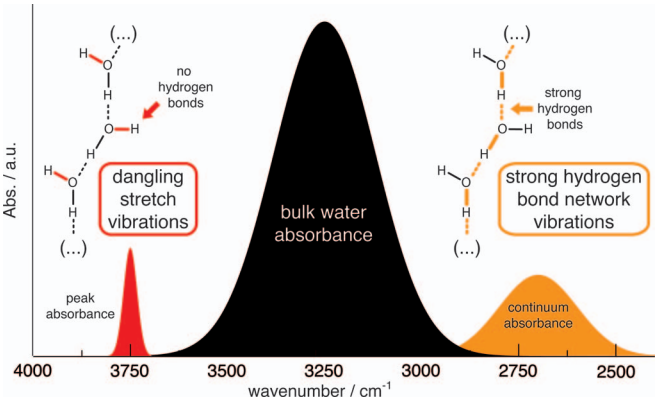

FIG. 4. Schematics of IR spectral ranges found to be characteristic for water wires in proteins. The bulk water absorption (black) masks any specific IR absorption between 3600 cm^{-1} and 2800 cm^{-1}. Between 3850 cm^{-1} and 3650 cm^{-1}, sharp absorbance peaks can be observed, coming from dangling O–H stretch vibrations. Between 2900 cm^{-1} and 2500 cm^{-1}, a broad continuum absorbance is observed, coming from combined stretch vibrations along the line of O–H bonds and hydrogen bonds.

the exact number of water molecules forming the water wire. We could confirm our earlier assumption from MM simulations that the N intermediate water wire in bR is formed out of three water molecules. This shows that, with the approach presented herein, we are now capable of directly and unambiguously determining the structure and dynamics of transient water wires based on FTIR spectra and protein crystal structures with missing functionally important water molecules. Our work paves the way for similar analyses of permanent or transiently formed water wires that serve as proton conducting pathways in other membrane proteins, such as PS II,[2–4] cytochrome C oxidase,[5,6] bacterial reaction center,[9,10] respiratory complex I,[8] channelrhodopsins,[17,18] human proton channels,[15,16] or viral proton channels.[20,21] Our results may also help to better understand the GPCR activation process, which appears to be coupled to protein-bound water molecule reorganization.[23–28] This work therefore contributes to the understanding of how protein internal water molecules reorganize and contribute to the structure, dynamics and function of membrane proteins in general. Furthermore, our approach can be used for monitoring transient water motifs appearing in confined nanoscale hydrophobic environments, and thus for research on nanotube-based molecular systems,[33,34,71] water-mediated ligand binding to proteins,[72] or molecular machines[73] in general.

ACKNOWLEDGMENTS

We would like to thank M. Elstner for helpful discussions. DFT calculations were performed on the HPC PURE cluster at the Biophysics Department of the Ruhr-University Bochum. SCC-DFTB QM/MM calculations were performed on the Partner Institute for Computational Biology High-Performance Computing cluster. S.W. is funded by a Chinese Academy of Sciences Fellowship for Young International Scientists. This work was supported by a grant from the National Natural Science Foundation of China Young Scientist Fund (Grant No. 31250110070). All molecular figures were prepared with PyMOL (Schrödinger, LLC).

[1] K. Gerwert, E. Freier, and S. Wolf, BBA-Bioenergetics **1837**, 606 (2014).
[2] Y. Umena, K. Kawakami, J.-R. Shen, and N. Kamiya, Nature (London) **473**, 55 (2011).
[3] B. C. Polander and B. A. Barry, Proc. Natl. Acad. Sci. U.S.A. **110**, 10634 (2013).
[4] K. Linke and F. M. Ho, BBA-Bioenergetics **1837**, 14 (2014).
[5] S. Iwata, C. Ostermeier, B. Ludwig, and H. Michel, Nature (London) **376**, 660 (1995).
[6] J. Koepke, E. Olkhova, H. Angerer, H. Müller, G. Peng, and H. Michel, BBA-Bioenergetics **1787**, 635 (2009).
[7] P. Goyal, J. Lu, S. Yang, M. R. Gunner, and Q. Cui, Proc. Natl. Acad. Sci. U.S.A. **110**, 18886 (2013).
[8] V. R. I. Kaila, M. Wikström, and G. Hummer, Proc. Natl. Acad. Sci. U.S.A. **111**, 6988 (2014).
[9] M. H. Stowell, Science **276**, 812 (1997).
[10] J. Koepke, E.-M. Krammer, A. R. Klingen, P. Sebban, G. M. Ullmann, and G. Fritzsch, J. Mol. Biol. **371**, 396 (2007).
[11] W. Junge, Science **308**, 642 (2005).
[12] N. Agmon, Chem. Phys. Lett. **244**, 456 (1995).
[13] P. Ball, Chem. Rev. **108**, 74 (2008).
[14] F. Garczarek and K. Gerwert, Nature (London) **439**, 109 (2005).
[15] I. S. Ramsey, Y. Mokrab, I. Carvacho, Z. A. Sands, M. S. P. Sansom, and D. E. Clapham, Nat. Struct. Mol. Biol. **17**, 869 (2010).
[16] A. Chamberlin, F. Qiu, S. Rebolledo, Y. Wang, S. Y. Noskov, and H. P. Larsson, Proc. Natl. Acad. Sci. U.S.A. **111**, E273 (2014).
[17] H. E. Kato, F. Zhang, O. Yizhar, C. Ramakrishnan, T. Nishizawa, K. Hirata, J. Ito, Y. Aita, T. Tsukazaki, S. Hayashi, P. Hegemann, A. D. Maturana, R. Ishitani, K. Deisseroth, and O. Nureki, Nature (London) **482**, 369 (2012).
[18] K. Eisenhauer, J. Kuhne, E. Ritter, A. Berndt, S. Wolf, E. Freier, F. Bartl, P. Hegemann, and K. Gerwert, J. Biol. Chem. **287**, 6904 (2012).
[19] K. Deisseroth, Nat. Methods **8**, 26 (2010).
[20] J. R. Schnell and J. J. Chou, Nature (London) **451**, 591 (2008).
[21] R. Acharya, V. Carnevale, G. Fiorin, B. G. Levine, A. L. Polishchuk, V. Balannik, I. Samish, R. A. Lamb, L. H. Pinto, and W. F. DeGrado, Proc. Natl. Acad. Sci. U.S.A. **107**, 15075 (2010).
[22] U. Kosinska Eriksson, G. Fischer, R. Friemann, G. Enkavi, E. Tajkhorshid, and R. Neutze, Science **340**, 1346 (2013).
[23] J. Standfuss, P. C. Edwards, A. D'Antona, M. Fransen, G. Xie, D. D. Oprian, and G. F. X. Schertler, Nature (London) **471**, 656 (2011).
[24] W. Liu, E. Chun, A. A. Thompson, P. Chubukov, F. Xu, V. Katritch, G. W. Han, C. B. Roth, L. H. Heitman, A. P. IJzerman, V. Cherezov, and R. C. Stevens, Science **337**, 232 (2012).
[25] H. Gutiérrez-de-Terán, A. Massink, D. Rodríguez, W. Liu, G. W. Han, J. S. Joseph, I. Katritch, L. H. Heitman, L. Xia, A. P. IJzerman, V. Cherezov, V. Katritch, and R. C. Stevens, Structure **21**, 2175 (2013).
[26] G. Fenalti, P. M. Giguere, V. Katritch, X.-P. Huang, A. A. Thompson, V. Cherezov, B. L. Roth, and R. C. Stevens, Nature (London) **506**, 191 (2014).
[27] S. Filipek, K. Palczewski, S. Yuan, and H. Vogel, Nat. Commun. **5**, 4733 (2014).
[28] T. E. Angel, M. R. Chance, and K. Palczewski, Proc. Natl. Acad. Sci. U.S.A. **106**, 8555 (2009).
[29] J. A. Ernst, R. T. Clubb, H.-X. Zhou, A. M. Gronenborn, and G. M. Clore, Science **267**, 1813 (1995).
[30] B. Yu, M. Blaber, A. M. Gronenborn, G. M. Clore, and D. L. D. Caspar, Proc. Natl. Acad. Sci. U.S.A. **96**, 103 (1999).
[31] S. Vaitheeswaran, H. Yin, J. C. Rasaiah, and G. Hummer, Proc. Natl. Acad. Sci. U.S.A. **101**, 17002 (2004).
[32] L. Liu, M. L. Quillin, and B. W. Matthews, Proc. Natl. Acad. Sci. U.S.A. **105**, 14406 (2008).
[33] G. Hummer, J. C. Rasaiah, and J. P. Noworyta, Nature (London) **414**, 188 (2001).
[34] K. S. Fangqiang Zhu, Biophys. J. **85**, 236 (2003).
[35] E. Freier, S. Wolf, and K. Gerwert, Proc. Natl. Acad. Sci. U.S.A. **108**, 11435 (2011).
[36] J. K. Lanyi, Annu. Rev. Physiol. **66**, 665 (2004).
[37] J. L. Spudich and K. H. Jung, *Handbook of Photosensory Receptors*, edited by W. R. Briggs and J. L. Spudich (Wiley-VCH, Weinheim 2004), pp. 1–24.
[38] V. A. Lórenz-Fonfría and H. Kandori, J. Am. Chem. Soc. **131**, 5891 (2009).
[39] S. Wolf, E. Freier, M. Potschies, E. Hofmann, and K. Gerwert, Angew. Chem., Int. Ed. **49**, 6889 (2010).
[40] T. Ohba, K. Kaneko, M. Endo, K. Hata, and H. Kanoh, Langmuir **29**, 1077 (2013).
[41] M. J. Frisch, G. W. Trucks, H. B. Schlegel *et al.*, Gaussian 09, Revision D.01, Gaussian, Inc., Wallingford, CT, 2009.
[42] See supplementary material at http://dx.doi.org/10.1063/1.4902237 for Figures S1–S8 and Table SI.
[43] X. Li and M. J. Frisch, J. Chem. Theory Comput. **2**, 835 (2006).
[44] G. B. Bacskay, Chem. Phys. **61**, 385 (1981).
[45] K. K. Irikura, R. D. Johnson, and R. N. Kacker, J. Phys. Chem. A **109**, 8430 (2005).
[46] B. R. Brooks, C. L. Brooks, A. D. Mackerell, L. Nilsson, R. J. Petrella, B. Roux, Y. Won, G. Archontis, C. Bartels, S. Boresch, A. Caflisch, L. Caves, Q. Cui, A. R. Dinner, M. Feig, S. Fischer, J. Gao, M. Hodoscek, W. Im, K. Kuczera, T. Lazaridis, J. Ma, V. Ovchinnikov, E. Paci, R. W. Pastor, C. B. Post, J. Z. Pu, M. Schaefer, B. Tidor, R. M. Venable, H. L. Woodcock, X. Wu, W. Yang, D. M. York, and M. Karplus, J. Comput. Chem. **30**, 1545 (2009).
[47] A. D. Mackerell, D. Bashford, M. Bellott, R. L. Dunbrack, J. D. Evanseck, M. J. Field, S. Fischer, J. Gao, H. Guo, S. Ha, D. Joseph-McCarthy, L. Kuchnir, K. Kuczera, F. T. K. Lau, C. Mattos, S. Michnick, T. Ngo, D. T. Nguyen, B. Prodhom, W. E. Reiher, B. Roux, M. Schlenkrich, J. C. Smith, R. Stote, J. Straub, M. Watanabe, J. Wiórkiewicz-Kuczera, D. Yin, and M. Karplus, J. Phys. Chem. B **102**, 3586 (1998).

[48]W. L. Jorgensen, J. Chandrasekhar, J. D. Madura, R. W. Impey, and M. L. Klein, J. Chem. Phys. **79**, 926 (1983).
[49]B. Schobert, L. S. Brown, and J. K. Lanyi, J. Mol. Biol. **330**, 553 (2003).
[50]A. T. Brünger and M. Karplus, Proteins **4**, 148 (1988).
[51]S. P. Balashov, BBA-Bioenergetics **1460**, 75 (2000).
[52]E. Tajkhorshid and S. Suhai, J. Phys. Chem. B **103**, 5581 (1999).
[53]E. Tajkhorshid, B. Paizs, and S. Suhai, J. Phys. Chem. B **103**, 4518 (1999).
[54]W. Im, S. Bernèche, and B. Roux, J. Chem. Phys. **114**, 2924 (2001).
[55]P. Schaefer, D. Riccardi, and Q. Cui, J. Chem. Phys. **123**, 014905 (2005).
[56]P. Goyal, N. Ghosh, P. Phatak, M. Clemens, M. Gaus, M. Elstner, and Q. Cui, J. Am. Chem. Soc. **133**, 14981 (2011).
[57]M. Elstner, D. Porezag, G. Jungnickel, J. Elsner, M. Haugk, T. Frauenheim, S. Suhai, and G. Seifert, Phys. Rev. B **58**, 7260 (1998).
[58]Yang, H. Yu, D. York, Q. Cui, and M. Elstner, J. Phys. Chem. A **111**, 10861 (2007).
[59]P. H. König, M. Hoffmann, T. Frauenheim, and Q. Cui, J. Phys. Chem. B **109**, 9082 (2005).
[60]C. L. Brooks and M. Karplus, J. Mol. Biol. **208**, 159 (1989).
[61]B. Hess, C. Kutzner, D. Van Der Spoel, and E. Lindahl, J. Chem. Theory Comput. **4**, 435 (2008).
[62]P. J. Steinbach and B. R. Brooks, J. Comput. Chem. **15**, 667 (1994).
[63]R. G. Gordon, J. Chem. Phys. **43**, 1307 (1965).
[64]D. A. McQuarrie, *Statistical Mechanics* (Harper and Row, New York, 1976).
[65]J.-P. Ryckaert, G. Ciccotti, and H. J. C. Berendsen, J. Comput. Phys. **23**, 327 (1977).
[66]H. Yu and Q. Cui, J. Chem. Phys. **127**, 234504 (2007).
[67]H. Luecke, B. Schobert, J.-P. Cartailler, H.-T. Richter, A. Rosengarth, R. Needleman, and J. K. Lanyi, J. Mol. Biol. **300**, 1237 (2000).
[68]H. Kandori, BBA-Bioenergetics **1460**, 177 (2000).
[69]D. Onidas, J. M. Stachnik, S. Brucker, S. Krätzig, and K. Gerwert, Eur. J. Cell Biol. **89**, 983 (2010).
[70]Z. Cao, Y. Peng, T. Yan, S. Li, A. Li, and G. A. Voth, J. Am. Chem. Soc. **132**, 11395 (2010).
[71]O. Byl, J.-C. Liu, Y. Wang, W.-L. Yim, J. K. Johnson, and J. T. Yates, J. Am. Chem. Soc. **128**, 12090 (2006).
[72]G. Hummer, Nat. Chem. **2**, 906 (2010).
[73]M. R. Panman, B. H. Bakker, D. den Uyl, E. R. Kay, D. A. Leigh, W. J. Buma, A. M. Brouwer, J. A. J. Geenevasen, and S. Woutersen, Nat. Chem. **5**, 929 (2013).